Demonstration of PMD Compensation by LDPC-Coded Turbo Equalization and Channel Capacity Loss Characterization Due to PMD and Quantization

L. L. Minkov, I. B. Djordjevic, H. G. Batshon, L. Xu, T. Wang, M. Cvijetic, and F. Kueppers

***Abstract*—Polarization-mode dispersion (PMD) compensation by low-density parity-check (LDPC) coded turbo equalization is experimentally demonstrated for a nonreturn-to-zero (NRZ) system operating at 10 Gb/s. This technique provides significant improvement of bit-error rate compared to the optimum threshold receiver. The channel capacity loss due to PMD and quantization is studied as well. It was found that the proposed PMD turbo equalizer is about 1.5 dB away from the theoretical limit.**

***Index Terms*—Channel capacity, equalization, low-density parity-check (LDPC) codes, polarization-mode dispersion (PMD) compensation.**

I. Introduction

POLARIZATION-MODE dispersion (PMD) and fiber nonlinearities are the major transmission impairments in high-speed optical transmission systems. PMD is time variant and stochastic in nature; hence, it is much more difficult to compensate for compared to chromatic dispersion. Different PMD compensation techniques have been proposed recently, including Viterbi equalizer, Bahl–Cocke–Jelinek–Raviv (BCJR) equalizer, and turbo equalizer [1]–[4].

In this letter, we study the performance of a PMD compensator based on low-density parity-check (LDPC) coded turbo equalization scheme. We demonstrate experimentally that it is an outstanding PMD compensation candidate. The purpose of the letter is twofold: 1) study of the error correction capabilities of the LDPC-coded PMD turbo equalizer and 2) determination of the channel capacity degradation due to PMD. The goal is to determine how far away the scheme under study is from the theoretical limit.

The PMD compensation scheme under study in this letter is composed of two components: the BCJR equalizer and the LDPC decoder. The BCJR equalizer itself serves several purposes: 1) partially reduces the inter-symbol interference (ISI) caused by differential group delay (DGD); 2) reduces the BER to that of the decoder threshold; and 3) calculates log likelihood ratios (LLRs) used as initial input to the decoder. The LDPC decoder has two main functions: 1) it performs the main BER correction and 2) it calculates extrinsic LLRs (difference between decoder input and output LLRs) and passes them to the BCJR equalizer. To enable the iteration of the extrinsic information between BCJR equalizer and LDPC decoder (iteration also known as *turbo equalization*), a special class of structured LDPC codes was employed. These are based on combinatorial objects known as *balanced incomplete block designs* (BIBDs) [5]. To verify the relevance of using that class of LDPCs for turbo equalization of PMD, extrinsic information transfer (EXIT) chart analysis [6] was used. For further details, the reader is referred to [7].

To study the degradation effect of PMD, the independent and identically distributed (i.i.d.) channel capacity is determined. (The i.i.d. refers to the distribution of the 0s and 1s of the information source.) The i.i.d channel capacity is a lower bound on the channel capacity, and can be achieved by implementing the best known techniques for detection, equalization, and coding. The calculation of the i.i.d. channel capacity follows the approach described in [8]. It consists of two steps: 1) determination of conditional probability density functions (pdfs) from experimentally collected histograms and 2) capacity calculation based on the forward step of the BCJR algorithm. We determine the i.i.d. channel capacity loss due to: 1) PMD; 2) A/D conversion; 3) inadequate channel memory assumption; and 4) quantization of LLRs.

Previous results [2] indicate that the LDPC-coded PMD turbo equalizer can be used for PMD-induced DGD compensation of up to 300 ps and acceptable complexity of the BCJR equalizer. Due to technical limitations (PMD emulator range), the experimental results in this letter are reported for DGDs up to 125 ps.

II. Experimental Setup, PMD Compensator, and Capacity Calculation

Fig. 1 shows the setup used for this experiment. A precoded test pattern was uploaded into a pulse generator (Anritsu MP1763C) via personal computer (PC) with GPIB interface. The 10-Gb/s nonreturn-to-zero (NRZ) signal was used to drive a zero chirp Mach–Zehnder modulator (UTP). Then the signal passed through PMD emulator (JDSU PE3), where a controlled amount of DGD was introduced. The distorted signal was mixed with a controlled amount of amplified spontaneous emission (ASE) noise with a 3-dB coupler. A modulated signal level was maintained at 0 dB while the ASE power level was changed to

Manuscript received May 7, 2007; revised August 7, 2007.

L. L. Minkov, I. B. Djordjevic, and H. G. Batshon are with the Department of Electrical and Computer Engineering, University of Arizona, Tucson, AZ 85721 USA (e-mail: ljubo@email.arizona.edu; ivan@email.arizona.edu; hbatshon@email.arizona.edu).

L. Xu and T. Wang are with NEC Labs of America, Princeton, NJ 08540 USA.

M. Cvijetic is with NEC Corporation of America, Herndon, VA 20171 USA.

F. Kueppers is with the College of Optical Sciences, University of Arizona, Tucson, AZ 85721 USA.

Color versions of one or more of the figures in this letter are available online at http://ieeexplore.ieee.org.

Digital Object Identifier 10.1109/LPT.2007.907636

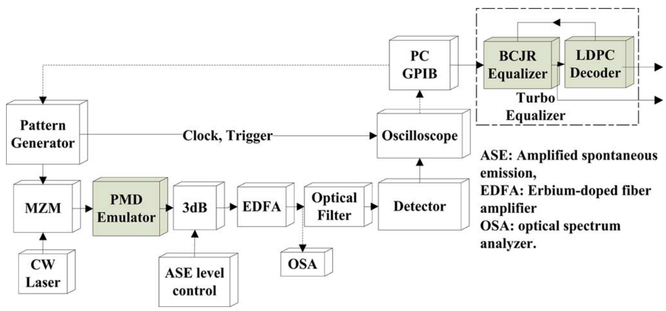

Fig. 1. Experimental setup.

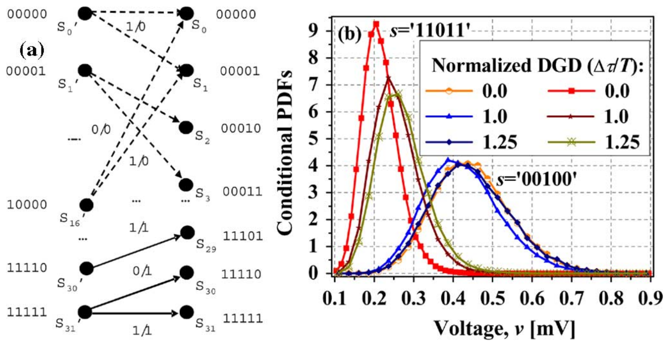

Fig. 2. (a) Trellis description $(2m+1=5)$. (b) Measured conditional pdfs for different DGDs.

obtain different optical signal-to-noise ratios (OSNRs). Next, the optical signal was preamplified (Optigain, Inc. 2000 series), filtered (JSDU 2-nm bandpass filter), followed by detection (Agilent 11982 A). An oscilloscope (Agilent DCA 86105A) triggered by the data pattern was used to acquire the samples. To maintain constant power of −6 dBm at the detector, a variable attenuator was used. Data was transferred via GPIB back to the PC, which served as an LDPC decoder.

As explained in a previous paper [9], the optical channel is described by discrete dynamical trellis and is modeled as an ISI channel with memory $2m+1$. Let $\boldsymbol{X}$ and $\boldsymbol{Y}$ denote the transmitted and the received sequences, respectively. The memory assumption means that a bit x_i is affected by the preceding $m(x_{i-m}, x_{i-m+1}, \cdot, x_{i-1})$ bits and the next $m(x_{i+1}, \ldots, x_{i+m})$ bits in the sequence. The BCJR equalizer operates on the channel trellis. A state is defined as $\boldsymbol{s} = (x_{i-m}, \cdot, x_i, x_{i+1}, \ldots, x_{i+m})$. At any moment of time the trellis is uniquely defined in terms of the triple {previous state, channel output, next state}. To completely describe the trellis transition, pdfs are required. They are calculated from the histograms of collected data. The pdf is defined as $p(y_j|\boldsymbol{s})$ (y_j is the sample that corresponds to x_j). Fig. 2(a) illustrates the trellis for memory $2m+1=5$. Fig. 2(b) shows the conditional pdfs of the received sample y for two states: $s =$ '11011' and '00100' and different values for DGD. The PDF mean for state $s =$ '11011' shifts to the right, with the increase of DGD. Due to the insufficient memory of the PMD compensator, the residual ISI becomes more significant as DGD increases. Clearly, the PDF curve becomes wider, and BER performance degrades when more DGD is introduced.

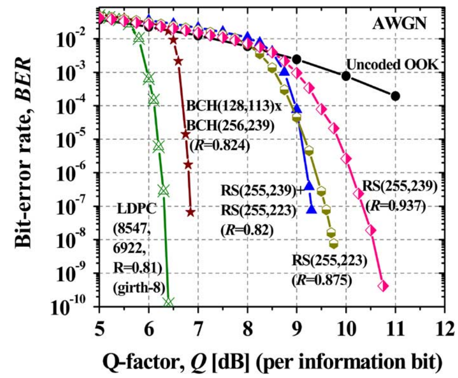

Fig. 3. Comparison between LDPC, RS, and turbo codes.

Assuming that the transmitted sequence $\boldsymbol{X}$ is independent and uniformly distributed, the information rate can be calculated from

$$I(\mathbf{Y};\mathbf{X}) = H(\mathbf{Y}) - H(\mathbf{Y}|\mathbf{X}) \tag{1}$$

where $H(\boldsymbol{U}) = \mathrm{E}(\log_2 P(\boldsymbol{U}))$ is the entropy of a random variable $\boldsymbol{U}$ and $\mathrm{E}(\cdot)$ is the mathematical expectation operator. The Shannon–McMillan–Brieman theorem states that

$$E\left(\log_2 P\left(\boldsymbol{Y}_1^n\right)\right) = \lim_{n\to\infty} (1/n) \log_2 P\left(\boldsymbol{Y}_1^n\right) \tag{2}$$

where $\boldsymbol{Y}_1^n = (Y_1, \ldots, Y_n)$. Thus, the information rate can be determined by calculating $\log_2(P(\boldsymbol{Y}_1^n))$, for sufficiently long sequence. This is done by using the forward step of the BCJR algorithm [8] (see also therein [6]). Another observation is that proper pdf calculation requires sufficiently long training sequences. The used sequence for this experiment consisted of a 8547-bit long sequence which was sent and received 128 times, totaling over 1 million bits.

To achieve optimal performance with iterative decoding, soft bit reliabilities are needed. That gives the BCJR equalizer a considerable advantage over the Viterbi equalizer. The LLRs provided by the BCJR equalizer are processed LDPC decoder implemented using the sum-product algorithm (SPA). The SPA's iterations are referred to as *inner iterations*. The passing of the extrinsic LLRs from the decoder to the equalizer is referred to as an *outer iteration*. Significant advantage of the proposed scheme over existing turbo equalization schemes [3], [10] is that it does not require the use of interleavers because it is based on LDPC codes. That reduces the time for processing and thus facilitates practical implementation at high speed. The LDPC codes used in this experiment are girth-8 codes designed using the concept of BIBDs [5].

Fig. 3 shows a comparison of BER performance of the proposed LDPC code against Reed–Solomon (RS), concatenated RS, and turbo-product codes. For the LDPC code rate of $R = 0.81$, 30 iterations in the SPA were used. At BER of 10^{-7} the LDPC code outperformed $R = 0.824$ turbo-product code by more than 0.5 dB, and $R = 0.82$ concatenated RS code by 3 dB.

III. Experimental Results and Conclusion

Fig. 4 shows experimental results for BER for different values of DGD $\Delta\tau$ normalized with the bit period T. The BCJR equalizer provided an improvement of 2.5 dB for DGD 0.75 compared to the memoryless maximum *a posteriori*

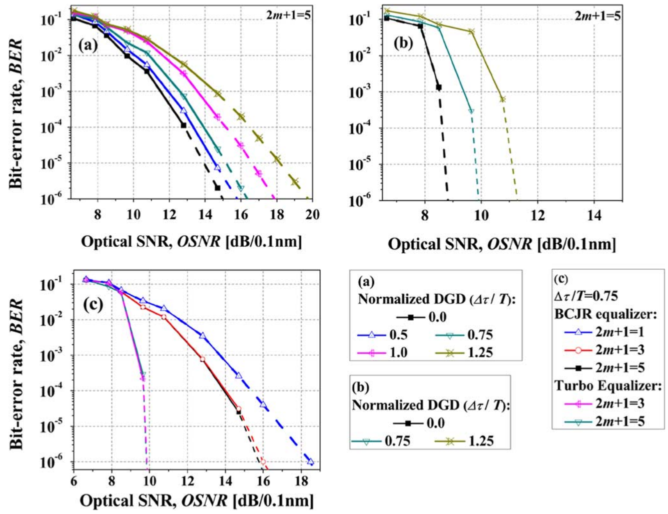

Fig. 4. BERs for different values of normalized DGD: (a) BCJR equalizer, (b) LDPC-coded turbo equalizer, and (c) BCJR/turbo equalizers for different memory assumptions.

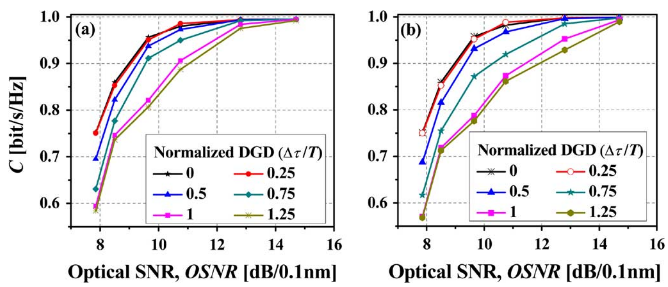

Fig. 5. Memory effects on i.i.d. channel capacity. (a) BER plots at memory $2m + 1 = 5$. (b) BER plots at memory $2m + 1 = 1$.

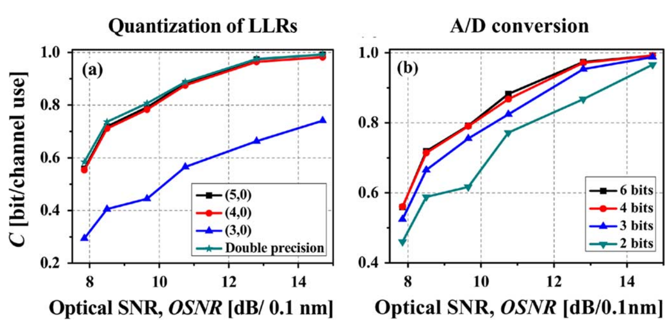

Fig. 6. Quantization effects influence on i.i.d. channel capacity (C). (a) LLR quantization. (b) A/D conversion.

probability (MAP) detector with trellis memory of $2m + 1 = 5$ and BER of 10^{-6}. After the LDPC decoder the coding gain improvement over MAP detector was 8.5 dB for the same BER and net effective gain of 7.6 dB (for 5 outer and 25 inner iterations). The penalty for DGD 1.25 is about 2.5 dB compared to DGD 0. Better improvements are expected at lower BERs. Note that for DGD of 125 ps an optimum threshold receiver enters the BER floor that is above the threshold of any practical FEC scheme.

Fig. 5 shows the experimental results for the i.i.d. capacity for different values of the trellis memory ($2m+1 = 5$ and $2m+1 = 1$). It is clear that the use of dynamic discrete model for the optical channel is needed to effectively reduce PMD effects.

Fig. 6 shows how the quantization effects influence the i.i.d. channel capacity loss. Fig. 6(a) studies quantization of the LLRs, while Fig. 6(b) studies the influence of A/D conversion. Let the real LLR be denoted by λ. Calculations for Fig. 5 were done with double precision numbers. For Fig. 6, a 2-tuple of integers (d_b, p_b) was used to represent the integer (with sign) and decimal part of λ, respectively [8]. For example, in (5,0) representation, 5 denotes the number of bits used to represent the integer part of λ and 0 represents the number of bits used for the decimal part. Fig. 6(a) demonstrates that (5,0) and (4,0) representations are very close to the double precision one. Significant i.i.d. channel capacity degradation is observed for the (3,0) case. From Fig. 6(b), we conclude that the i.i.d. channel capacity is less sensitive to A/D quantization compared to LLR quantization. Although significant loss is noticed for the (3,0) case, it is not as severe as in the LLR case.

In conclusion, we experimentally demonstrate that LDPC-coded turbo equalization is an outstanding PMD compensation candidate. Major advantages over the currently employed PMD compensating schemes are: 1) high regularity of the parity check matrix leads to simplified practical implementation; 2) use of interleavers is not required, which decreases processing delay; and 3) no error-floor phenomenon is exhibited by this class of LDPC codes [2], [11]. i.i.d. channel capacity loss due to PMD, quantization, inaccurate channel assumption, and ASE noise is studied. It is found that 4-bit integer representation is sufficient for both LLR and A/D quantizations. It is found that there is 2.5-dB power penalty for 125-ps DGD over the undistorted case at BER 10^{-6}. The LDPC-coded turbo equalization scheme considered in this letter is approximately 1.5 dB away from the i.i.d. channel capacity. In order to come closer to the theoretical limit, longer LDPC codes have to be employed. This can be achieved at the expense of longer decoding delay and increased complexity.

References

[1] F. Buchali and H. Bülow, "Correlation sensitive Viterbi equalization of 10 Gb/s signals in bandwidth limited receivers [optical receivers]," in *Proc. OFC 2005*, Anaheim, CA, 2005, Paper F020.

[2] I. B. Djordjevic, H. G. Batshon, M. Cvijetic, L. Xu, and T. Wang, "PMD compensation by LDPC coding based turbo equalization," *IEEE Photon. Technol. Lett.*, vol. 19, no. 15, pp. 1163–1165, Aug. 1, 2007.

[3] M. Jäger, T. Rankl, J. Speidel, H. Bülow, and F. Buchali, "Performance of turbo equalizers for optical PMD channels," *J. Lightw. Technol.*, vol. 24, no. 3, pp. 1226–1236, Mar. 2006.

[4] L. Bahl, J. Cocke, F. Jelinek, and J. Raviv, "Optimal decoding of linear codes for minimizing symbol error rate," *IEEE Trans. Inf. Theory*, vol. IT-20, no. 2, pp. 284–287, Mar. 1974.

[5] I. Anderson, *Combinatorial Designs and Tournaments*. Oxford, U.K.: Oxford Univ. Press, Apr. 1997.

[6] S. ten Brink, "Convergence behavior of iteratively decoded parallel concatenated codes," *IEEE Trans. Commun.*, vol. 49, no. 10, pp. 1727–1737, Oct. 2001.

[7] I. B. Djordjevic, M. Cvijetic, L. Xu, and T. Wang, "Proposal for beyond 100-Gb/s optical transmission based on bit-interleaved LDPC-coded modulation," *IEEE Photon. Technol. Lett.*, vol. 19, no. 12, pp. 874–876, Jun. 15, 2007.

[8] I. B. Djordjevic, N. Alic, G. C. Papen, and S. Radic, "Determination of achievable information rates (AIRs) of IM/DD systems and AIR loss due to chromatic dispersion and quantization," *IEEE Photon. Technol. Lett.*, vol. 19, no. 1, pp. 12–14, Jan. 1, 2007.

[9] I. Djordjevic and B. Vasic, "Nonlinear BCJR equalizer for suppression of intrachannel nonlinearities in 40 Gb/s optical communications systems," *Opt. Express*, vol. 14, pp. 4625–4635, May 2006.

[10] C. Douillard, A. Picart, P. Didier, M. Jézéquel, C. Berrou, and A. Glavieux, "Iterative correction of intersymbol interference: Turbo-equalization," *Eur. Trans. Telecommun.*, vol. 6, pp. 507–511, Sep./Oct. 1995.

[11] I. B. Djordjevic *et al.*, "Low-density parity-check codes for 40 Gb/s optical transmission systems," *IEEE J. Sel. Topics Quantum Electron.*, vol. 12, no. 4, pp. 555–562, Jul./Aug. 2006.